RESEARCH PAPER

Anti-inflammatory effects of dimemorfan on inflammatory cells and LPS-induced endotoxin shock in mice

Y-H Wang[1], Y-C Shen[2,3,10], J-F Liao[4,10], C-H Li[5,6], C-Y Chou[7], K-T Liou[8] and Y-C Chou[1,4,9]

[1]Department of Pharmacy, Taipei Veterans General Hospital, Taipei, Taiwan; [2]National Research Institute of Chinese Medicine, Taipei, Taiwan; [3]College of Life Science, Institute of Biomedical Sciences, National Chung-hsing University, Taichung, Taiwan; [4]School of Medicine, Institute of Pharmacology, National Yang-Ming University, Taipei, Taiwan; [5]Taipei Veterans General Hospital, Taipei, Taiwan; [6]School of Medicine, National Yang-Ming University, Taipei, Taiwan; [7]Intensive Care Unit, Department of Internal Medicine, Taipei Veterans General Hospital, Taipei, Taiwan; [8]College of Education, Graduate Institute of Sport Coaching Science, Chinese Culture University, Taipei, Taiwan and [9]School of Pharmacy, Taipei Medical University, Taipei, Taiwan

Background and purpose: Dimemorfan (a σ_1 receptor agonist) showed neuroprotective properties in animal models of inflammation-mediated neurodegenerative conditions, but its effects on inflammatory cells and systemic inflammation remain unclear.

Experimental approach: The effects of dimemorfan on phorbol-12-myristate-13-acetate (PMA)- and N-formyl-methionyl-leucyl-phenylalanine (fMLP)- induced neutrophils and lipopolysaccharide (LPS)-activated microglial cells, as well as LPS-induced endotoxin shock in mice were elucidated.

Key results: Dimemorfan decreased PMA- and fMLP-induced production of reactive oxygen species (ROS) and CD11b expression in neutrophils, through mechanisms independent of σ_1 receptors, possibly by blocking ROS production and G-protein-mediated intracellular calcium increase. Dimemorfan also inhibited LPS-induced ROS and nitric oxide (NO) production, as well as that of monocyte chemoattractant protein-1 and tumour necrosis factor-alpha (TNF-α), by inhibition of NADPH oxidase (NOX) activity and suppression of iNOS up-regulation through interfering with nuclear factor kappa-B (NF-κB) signalling in microglial cells. Treatment in vivo with dimemorfan (1 and 5 mg kg^{-1}, i.p., at three successive times after LPS) decreased plasma TNF-α, and neutrophil infiltration and oxidative stress in the lung and liver.

Conclusions and implications: Our results suggest that dimemorfan acts via σ_1 receptor-independent mechanisms to modulate intracellular calcium increase, NOX activity, and NF-κB signalling, resulting in inhibition of iNOS expression and NO production, and production of pro-inflammatory cytokines. These effects may contribute its anti-inflammatory action and protective effects against endotoxin shock in mice.

British Journal of Pharmacology (2008) **154**, 1327–1338; doi:10.1038/bjp.2008.202; published online 26 May 2008

Introduction

Dimemorfan (D-3-methyl-N-methylmorphinan), an antitussive and sigma-1 (σ_1) receptor agonist, has been reported to display σ_1 receptor-mediated neuroprotective properties including an anticonvulsant effect by modulation of the activating protein-1 (AP-1) transcription factor (Chou et al., 1999; Shin et al., 2005), an anti-amnesic effect on scopolamine- and β-amyloid peptide-induced memory impairment in mice (Wang et al., 2003), and a protective effect against ischaemic stroke in rats through reducing glutamate-induced excitotoxicity to suppress the initiation of inflammation-related events, such as neutrophil infiltration and microglia activation, and signals, such as nuclear factor kappa-B (NF-κB) activation, as well as induction of oxidative and nitrosative stresses, leading to reductions in tissue damage

Correspondence: Dr Y-C Chou, Department of Pharmacy, Taipei Veterans General Hospital, 201, Shih-Pai Road, Section 2, Shih-Pai, Taipei 112, Taiwan.
E-mail: ycchou@vghtpe.gov.tw and Dr Y-C Shen, National Research Institute of Chinese Medicine, 155-1 Li-Nung Street, Section 2, Shih-Pai, Taipei 112, Taiwan.
E-mail: yuhcs@nricm.edu.tw
[10]These two authors contributed equally to this work.
Received 18 February 2008; revised 10 March 2008; accepted 14 April 2008; published online 26 May 2008

and cell death (Shen *et al.*, 2008). Similarly, numerous studies have shown that σ_1 receptor ligands display protective properties in animal models of cerebral ischaemia (Ajmo *et al.*, 2006) and exhibit potent anti-inflammatory properties by modulation of cytokine production (Bourrié *et al.*, 2002, 2004) and NO synthesis (Gannon *et al.*, 2001) in macrophages and mice.

Inflammation is an important host defense mechanism against harmful factors such as invading pathogens, unwanted chemicals, damaged tissue, or diseases and allows elimination of these factors to maintain body health. To fulfil this purpose, a variety of immune cells are mobilized to neutralize and dispose of those factors. In the peripheral immune system, leukocytes, especially neutrophils and mononuclear cells, play key roles in mediating acute inflammatory responses (Williams, 1994; Kodama *et al.*, 2007). A similar inflammation process also occurs in the CNS where glial cells, especially microglial cells, and/or neutrophils undergoing activation in response to stimuli, infiltrate and accumulate in damaged tissues for pathogen clearance and tissue recovery (Williams, 1994; Ghoshal *et al.*, 2007). Unfortunately, loss of control or persistence of the inflammatory process, even when the inflammation-provoking stimulus is abolished, is known to mediate the progression of brain damage in a number of neurodegenerative diseases such as Alzheimer's disease, Parkinson's disease, seizures, and stroke (Rong and Baudry, 1996; Muir *et al.*, 2007; Rogers *et al.*, 2007; Van Eldik *et al.*, 2007). This inflammation-mediated damage may be attributed to over-production of potentially toxic mediators such as reactive oxygen species (ROS) and NO by pro-inflammatory proteins (NADPH oxidase (NOX), cyclooxygenase 2 and inducible NO synthase (iNOS)), pro-inflammatory cytokines, and excitotoxins predominantly through activation of NF-κB (Rong and Baudry, 1996; Mattson and Camandola, 2001; Williams *et al.*, 2006). Therefore, therapeutic suppression of inflammation would be of potential benefit in the treatment of several neurodegenerative diseases (Klegeris *et al.*, 2007) in addition to many inflammatory disorders (Nathan, 2002).

Although previous studies have demonstrated that dimemorfan exerts its neuroprotective effects through activation of σ_1-receptors, the effects of dimemorfan on inflammatory cells and systemic inflammation remain unclear. Therefore, we used two acute inflammation-related cellular models: (1) activation of human neutrophils by receptor-mediated (for example, *N*-formyl-methionyl-leucyl-phenylalanine; fMLP) and non-receptor-mediated (for example, phorbol-12-myristate-13-acetate; PMA) induction of ROS production and Mac-1 (CD11b/CD18) upregulation, and (2) LPS-induced production of NO, ROS, and pro-inflammatory cytokines, as well as iNOS expression and NF-κB signalling in the murine microglial cell line, BV2, to evaluate the anti-inflammatory effects of dimemorfan and the possible mechanisms of its actions in this study. Furthermore, LPS-induced endotoxin shock in mice, a model of systemic inflammation (Jiau *et al.*, 2006), was used to examine the *in vivo* activity of dimemorfan. Our results demonstrated that dimemorfan exhibits anti-inflammatory properties through σ_1-receptor independent mechanism(s) by inhibiting the production of NOX-dependent ROS and iNOS-dependent NO, as well as that of

pro-inflammatory cytokines, probably via modulation of NF-κB signalling in activated inflammatory cells. These actions may account for its protective effect against endotoxin shock in mice.

Materials and methods

Preparation of neutrophils and microglial cell culture
Our Institutional Review Board in accordance with international guidelines approved all experimental protocols performed in this study. Human neutrophils were obtained by venepuncture from adult healthy volunteers and collected into syringes containing heparin ($20\,U\,mL^{-1}$ blood) according to our previous report (Shen *et al.*, 2003). Neutrophils were isolated by the Ficoll (Histopaque 1077; Sigma-Aldrich, USA) gradient centrifugation method, followed by lysis of contaminating erythrocytes. The preparation contained more than 95% neutrophils, as estimated by counting 200 cells under a microscope, after Giemsa (Sigma-Aldrich) staining. In all cases, except where indicated, neutrophils were pretreated with test compounds at concentrations ranging from $1–50\,\mu M$ in HBSS for 20 min at $37\,°C$. The murine microglial cell line (BV2) was cultured in Dulbecco's modified Eagle medium (DMEM; Gibco, Grand Island, NY, USA) supplemented with 5% fetal bovine serum (Hyclone, Logan, UT, USA) as in our previous report (Wang *et al.*, 2006).

Measurement of ROS production
ROS production by neutrophil cells was measured as described in our previous study (Shen *et al.*, 2003). Briefly, after incubation with the test drug, a lucigenin ($50\,\mu M$)-preloaded neutrophil cell suspension ($1 \times 10^7\,cells\,mL^{-1}$, $50\,\mu L$) was stimulated by adding $50\,\mu L$ PMA ($0.2\,\mu M$) or fMLP ($1\,\mu M$). The chemiluminescence was monitored during a 30-min observation period using a microplate luminometer reader (Orion, Berthold DS, Tforzheim, Germany) and the results are presented as relative light units (RLU). Peak levels of RLU were recorded to calculate the 50% inhibitory concentration (IC_{50}) of the test drug. For the measurement of intracellular ROS production by BV2 cells, flow cytometry was used according to our previous report (Shen *et al.*, 1998). Briefly, BV2 ($2 \times 10^6\,cells\,mL^{-1}$) were incubated at $37\,°C$ for 20 min with $20\,\mu M$ of 2′,7′-dichlorofluorescin diacetate. After labelling, cells were treated with the test drug for 20 min followed by stimulation with LPS ($0.5\,\mu g\,mL^{-1}$). Production of intracellular H_2O_2 was then determined 24 h later by flow cytometry (FACSCalibur; Becton Dickinson, San Jose, CA, USA) with emission at 525 nm (FL1). Data are expressed as mean channel fluorescence (MCF) of each sample as calculated by the CellQuest software (Becton Dickinson).

Measurement of Mac-1 (CD11b/CD18) expression upregulated by PMA or fMLP
Mac-1 expression was analysed according to our previous study (Shen *et al.*, 1999). Briefly, after pretreatment with the test drug for 20 min, a neutrophil suspension

$(2 \times 10^6 \, \text{cells} \, \text{mL}^{-1})$ was stimulated with PMA (0.2 μM) or fMLP (1 μM) for 20 min. Cells were then pelleted and resuspended in 1 mL of ice-cold phosphate-buffered saline (PBS) containing 10% heat-inactivated fetal bovine serum (FBS) and 10 mM NaN_3. For staining of Mac-1, all subsequent steps were carried out in an ice bath. Cells were incubated in the dark for 60 min with fluorescein isothiocyanate (FITC)-conjugated anti-Mac-1 antibody (mouse anti-human CD11b, class immunoglobulin G_1 (IgG_1); BD Biosciences Pharmingen, San Diego, CA, USA) or a non-specific mouse antibody (class IgG_1, Sigma-Aldrich) as a negative control. After two washes with PBS containing 5% FBS, stained cells were resuspended in flow cytometer sheath fluid (Becton Dickinson) containing 1% paraformaldehyde and analysed by flow cytometry for Mac-1 expression. Data are expressed as the MCF for each sample as calculated by CellQuest software (Becton Dickinson).

Determination of intracellular calcium concentration ($[Ca^{2+}]_i$)

Neutrophils ($2 \times 10^7 \, \text{cells} \, \text{mL}^{-1}$) were preloaded with 5 μM 1-[2-(5-carboxyoxal-2-yl)-6-amino-benzofuran-5-oxyl]-2-(2′-amino-5′-methylphenoxy-ethane-N,N,N′,N′-tetraacetic acid acetoxy-methylester (fura-2 AM, Molecular Probes, Eugene, OR, USA) at 37 °C for 45 min, washed twice, and resuspended at $2 \times 10^6 \, \text{cells} \, \text{mL}^{-1}$ in calcium-free HBSS containing the test drug or vehicle control. After pretreatment for 20 min, 1 mL of the cell suspensions from each sample and 1 mL of HBSS containing 2 mM Ca^{2+} were transferred to individual cuvettes and gently mixed with a micromagnetic stirrer at 37 °C for 5 min before the addition of fMLP (1 μM) or the G-protein activator–AlF_4^- (10 mM NaF plus 30 μM $AlCl_3$), or a releaser of calcium from intracellular stores–thapsigargin (10 μM). The fluorescence of fura-2-loaded cells was measured by a spectrofluorometer (Hitachi F-4500, Tokyo, Japan) with excitation at 340 and 380 nm and emission at 510 nm. The intracellular calcium concentration for each sample was calculated from the ratio of emission versus excitation as previously described (Shen et al., 1999).

Measurement of NADPH oxidase (NOX) activity

NOX activity in the cell free system was measured as described previously (Wang et al., 2006). Test drugs were added to the wells of a bioluminescence plate and incubated with 50 μg of cell homogenate for 20 min at 37 °C in the dark. O_2^- production was stimulated with 200 μM NADPH in the presence of lucigenin (50 μM), and the chemiluminescence was monitored every 5 s for 30 min, after which the AUC (area under the curve) was calculated to determine NOX activity.

Measurement of scavenging capacity on 1,1-diphenyl-2-picrylhydrazyl (DPPH) radicals and reactive oxidants

The scavenging effects of dimemorfan on DPPH free radicals and reactive oxidants produced by xanthine/xanthine oxidase system were examined as described previously (Wang et al., 2004b). The DPPH solution (200 μL, at a final concentration of 200 μM in methanol) was added to 10 μL of diluted drugs in each well of a 96-well microplate, and the resulting solution was allowed to react for 30 min in the dark at room temperature. The absorbance (A517 OD units) is defined as the optical density (OD) measured at 517 nm caused by the DPPH radical as determined using a microplate-spectrophotometer (PowerWave XS, BioTek, Winooski, Vermont, USA). The radical-scavenging capacity is expressed as the change in the OD_{517} over 30 min. For ROS production, we used the xanthine oxidase-catalysed oxidation of xanthine to produce uric acid and both O_2^- and H_2O_2. The generation of these oxidants was performed in 1 mL PBS containing xanthine (160 mM) and xanthine oxidase (20 mM). The reaction was monitored both by the reduction of cytochrome c (0.5 mg mL^{-1}) at 550 nm and the production of uric acid at 290 nm over 5 min using a spectrophotometer (Hitachi Ltd, Tokyo, Japan).

Detection of cytokine production by intracellular immunofluorescence staining

The positively stained cell population (%) and intensity (MCF) of cytokine-producing microglial cells were determined as described (Di Francesco et al., 1999; Falchetti et al., 2001) with some modifications. Briefly, LPS (0.5 μg mL^{-1})-stimulated cells were fixed in 4% paraformaldehyde for 20 min and resuspended in PBS containing 0.5% BSA, 0.01% NaN_3, and 0.3% saponin (Sigma-Aldrich). Then phycoerythrin-conjugated anti-mouse monocyte chemoattractant protein-1 (MCP-1) or FITC-conjugated anti-mouse TNF-α (Biolegend, Camino Santa, CA, USA) was added for 30 min at 4 °C. As negative controls, aliquots of cell suspensions were incubated with an irrelevant isotype-matched monoclonal antibody (mAb) conjugated to the same fluorochrome as the sample. After washing three times with PBS containing 0.5% BSA and 0.01% NaN_3, cells was resuspended in sheath fluid for the cytofluorimetric analysis by flow cytometry (FACSCalibur, Becton Dickinson, Mountain View, CA, USA).

Measurement of nitrite

The production of NO by BV2 cells was determined by the accumulation of nitrite in the culture medium, 24 h after stimulation with LPS (0.5 μg mL^{-1}), using the Griess reagent as described in our previous report (Wang et al., 2006).

Western immunoblot analysis of iNOS, NFκB p65, and IκBα

Equal amounts of protein (50 μg) at different time points from samples treated with LPS (0.5 μg mL^{-1}). with or without dimemorfan pre-treatment (10–20 μM) were subjected to sodium dodecylsulphate polyacrylamide gel electrophoresis (SDS-PAGE) and electro-transferred to a hydrophobic polyvinylidene difluoride (PVDF) membrane. After blocking with 5% nonfat milk in PBS containing 0.05% Tween 20 (PBST) at 4 °C for 1 h, the membrane was washed three times with PBST and incubated overnight at 4 °C with an antibody against iNOS (BD Biosciences Pharmingen, San Diego, CA, USA), IκBα, NFκB p65 (BD Transduction Laboratories, San Diego, CA, USA), and phospho-NFκB p65 (Cell Signaling Technology, Beverly, MA, USA) at a properly titrated dilution

(1:1000–2500). After additional washes with PBST, the membrane was incubated with a second antibody IgG conjugated with horseradish peroxidase (Santa Cruz Biotechnology, Santa Cruz, CA, USA) for 1 h at room temperature. The immunoblot on the membrane was visible after development with an enhanced chemiluminescence (ECL) system (Perkin-Elmer, Wellesley, MA, USA) and was quantitated using an image program (Multi Gauge *v*2.2 software, Fujifilm, Tokyo, Japan).

Transient transfection of NF-κB reporter gene and luciferase assay
Transfection of the NF-κB reporter gene (pNFκB-Luc Vector, BD Biosciences Clontech, Palo Alto, CA, USA) into BV2 cells was performed using the CLONfectin transfection reagent (BD Biosciences Clontech). BV2 cells (3×10^5 per well in a 12-well plate) were transfected with 1 μg of the NF-κB reporter construct and 0.5 μg of the β-galactosidase reporter system (Promega Corporation, Madison, WI, USA) mixed with CLONfectin (1.5 μg). After 48 h, cells were harvested, and a luciferase assay was performed using Luciferase Reporter Assay Kits as described by the manufacturer (BD Biosciences Clontech). To determine the effect of dimemorfan on LPS-induced NF-κB activity, cells were pretreated with dimemorfan for 20 min before treatment with LPS ($0.5 \, \mu g \, mL^{-1}$) and incubated for 6 h prior to harvesting cells for the luciferase assay. Transfection assays were performed three times in duplicate.

LPS-induced endotoxin shock in mice
The ICR mice (25–30 g) were divided into three groups including endotoxin shock (LPS only), endotoxin shock with dimemorfan treatment and control (drug free). Endotoxin shock was induced by LPS ($70 \, mg \, kg^{-1}$, i.p.). Dimemorfan (1 and $5 \, mg \, kg^{-1}$, i.p.) was given three times successively, at 30 min, 6 and 12 h after LPS administration and the mice monitored for 48 h.

Measurement of plasma TNF-α concentration. Blood samples (0.5 mL) were collected using animal lancet (Goldenrod, Mineola, NY, USA) for cheek-pouch (submandibular) blood sampling at 6 and 12 h after the injection of LPS for measurement of the TNF-α concentration in plasma by an enzyme-linked immunoadsorbent assay (mouse TNF-α ELISA Kit, Genzyme Co., Cambridge, MA, USA).

Measurement of neutrophil infiltration and oxidative stress by immunohistochemical staining. At 48 h after LPS, animals were anaesthetized with sodium pentobarbital and then transcardially perfused with saline, followed by 4% paraformaldehyde in PBS. The lung and liver were removed, postfixed overnight in a solution containing 4% paraformaldehyde and 4% sucrose in PBS, and then cryoprotected in solutions containing 10, 15, and 20% sucrose in PBS for 1 day each. The tissues were then embedded in Tissue-Tek Optimal Cutting Temperature (OCT) compound (Sakura Finetek, Torrance, CA, USA) and frozen in liquid nitrogen. The tissue was serially sectioned (20 μm) by a cryostat (Microm HM560, Walldorf, Heidelberg, Germany). The

sliced tissues were fixed in a solution containing 4% paraformaldehyde and 4% sucrose in PBS for 15 min, permeabilized with 0.3% Triton-X in PBS for 10 min, treated with 10% donkey serum for 15 min in PBS containing 0.3% Triton X-100 to block non-specific binding, and then were randomly selected for incubation with first antibodies against a neutrophil marker myeloperoxidase (MPO, 1:50, Abcam, Cambridge, UK). After washing twice with PBST for 30 min, sections were incubated with FITC-conjugated second antibodies (1:100, Jackson Lab, Bar Harbor, ME, USA) in PBS containing 3% albumin for 1 h, and then washed twice again for 30 min each. We also used the appropriate neutralizing peptides or by omitting primary antibody during the staining procedure to check the specificity of the staining. All coverslips were mounted with Vectashield Mounting Medium (Vector Laboratories, Burlingame, CA, USA) containing an appropriate dilution of 4′,6-diamidino-2-phenylindole (DAPI) to counterstain DNA in the nuclei. The sections were examined using a laser-scanning confocal microscope (Leica DM IRBE microscope, TCS SPII confocal scanner; Leica Microsystems, Heidelberg, Germany). In some experiments, hydroethidium (HEt, Molecular Probes, Eugene, OR, U.S.A.), at $27 \, mg \, kg^{-1}$ in 200 μL water, was given i.p. to animals just before injection of LPS. HEt is oxidized by superoxide to ethidium (EB, red fluorescence) which can be detected by fluorescence microscopy as described (Shen *et al.*, 2008).

Quantification of the immunopositively stained cells. The distribution and numbers of immunopositively stained cells were determined, and averaged in the entire field of the image ($146 \times 146 \, \mu m^2$) after they had randomly been taken from six different non-overlapping regions sampled under high magnification ($\times 63$ objective).

Statistical analysis
All data in the text, tables, and figures are given as the mean ± s.e.m. Data were analysed by a two-tailed *t*-test or one-way analysis of variance (ANOVA) followed by the *post hoc* Student-Newman-Keuls *t*-test for multiple comparisons. The concentration dependence of each drug was analysed by a simple linear regression analysis of response levels against concentrations of the drug and tested the slope of the regression line against 0 by Student's *t*-test. Values of $P < 0.05$ were considered significant.

Materials
Dimemorfan, a gift from Astellas Pharma Inc., (Tokyo, Japan) was dissolved in water as stock solutions of 10 mM. A σ_1 receptor antagonist BD1047 was purchased from Tocris (Avonmouth, UK). All other compounds, except where specifically indicated, were purchased from Sigma-Aldrich (St Louis, MO, USA) and dissolved in dimethyl sulphoxide (DMSO). The final concentration of DMSO in the reaction buffer was less than 0.25%, which showed no significant cytotoxicity or biological activity when compared with drug-free samples as shown in our previous report (Wang *et al.*, 2006).

Results

Effects on fMLP- and PMA-induced ROS production in human neutrophils

In this study, we used fMLP (a receptor-mediated activator) and PMA (a direct protein kinase C activator) to stimulate ROS production in human neutrophils that was almost 20-fold higher than the resting control as estimated by the lucigenin-amplified chemiluminescence. Dimemorfan (5–20 μM) inhibited both fMLP- and PMA-induced ROS production in a concentration-dependent manner (one-way ANOVA, $P < 0.05$) and was relatively more potent in inhibiting fMLP-induced ROS production with an IC_{50} value of 7.0 μM (Table 1). To elucidate whether activation of σ_1 receptors was involved in the inhibitory effect on ROS production by dimemorfan, other σ_1 receptor ligands including an agonist (dextromethorphan) and an antagonist (BD1047) were studied. The results showed that these σ_1 receptor ligands both displayed different effects in this assay with the potency rank order as dimemorfan > BD1047 > dextromethorphan. Furthermore, the inhibitory effects of dimemorfan were potentiated by combination with BD1047 (Table 1), suggesting that σ_1 receptor activation was not directly involved in the inhibitory effect on ROS production, exerted by dimemorfan.

Scavenging effects on DPPH free radicals and reactive oxidants

To test whether dimemorfan exerted a direct free radical-scavenging capacity, the scavenging effects of dimemorfan on DPPH free radicals and reactive oxidants produced by xanthine/xanthine oxidase system were examined. The results showed that dimemorfan (10–50 μM) did not display significant activity in scavenging free radicals by these two systems (data not shown).

Effects on fMLP- and PMA-induced Mac-1 expression in human neutrophils

As shown in Figure 1, PMA and fMLP induced significant increases in the firm adhesion molecule Mac-1 to around 2.4- and 1.5-fold of the control, respectively. Dimemorfan

Figure 1 Effect of dimemorfan on Mac-1 up-regulation in human peripheral neutrophils. Mac-1 up-regulation in neutrophils (2×10^6 cells mL^{-1}) pre-treated with solvent (activator only) or 5–20 μM dimemorfan (activator + D5–20) were stimulated with one of two activators, phorbol-12-myristate-13-acetate (PMA, 0.2 μM) or N-formyl-methionyl-leucyl-phenylalanine (fMLP, 1 μM) for 20 min. After incubation with fluorescein isothiocyanate-conjugated anti-Mac-1 antibody, Mac-1 expression on cells were measured by flow cytometry and expressed as the mean channel fluorescence (MCF). Staurosporine (+ stau), a protein kinase C inhibitor, was used as a positive control. Data are expressed as the mean ± s.e.m. ($n = 3$–5 for each group). *$P < 0.05$, compared with the corresponding activator only group.

significantly suppressed Mac-1 upregulation both in PMA- and fMLP-activated groups (Figure 1, one-way ANOVA, $P < 0.05$). Pre-treatment with staurosporine (0.2 μM), a non-specific protein kinase C inhibitor, completely prevented Mac-1 upregulation induced by PMA or fMLP (Figure 1, one-way ANOVA, $P < 0.05$).

Effect on intracellular calcium concentration

We examined whether net increase in intracellular calcium concentration induced by fMLP (a receptor-mediated activator), AlF_4^- (a G-protein activator), and thapsigargin (an intracellular calcium mobilizer) in neutrophils can be modulated by dimemorfan. The results revealed that dimemorfan decreased intracellular calcium concentration induced by fMLP and AlF_4^- but not that induced by thapsigargin (Figure 2). Besides, dimemorfan was more effective in the inhibition of fMLP- than AlF_4^--induced increase in intracellular calcium concentration (Figure 2).

Effects on NO and ROS production in microglial cells

To further study the effect of dimemorfan on immune cell types resident in the brain, NO and ROS production in LPS-activated BV2 cells (microglial cells from the murine brain) was examined after pretreatment with dimemorfan (10–20 μM) for 20 min. LPS (0.5 μg mL^{-1}) stimulated ROS production to around 2.7-fold of the vehicle control and NO production to around 33 μM at 24 h after LPS stimulation (Figure 3). Non-activated microglial cells released no detectable amounts of NO (Figure 3). Dimemorfan (10–20 μM) significantly suppressed LPS-induced ROS and NO production

Table 1 Summary of the IC_{50} values of dimemorfan and some σ-receptor ligands; inhibition of ROS production induced by PMA- or fMLP in human neutrophils

Treatment	IC_{50} (μM)	
	PMA	fMLP
Dimemorfan	16.7 ± 3.6	7.0 ± 0.6[†]
BD1047	26.5 ± 4.0*	20.7 ± 0.6*
Dimemorfan + BD1047 (20 μM)	12.6 ± 3.9	5.1 ± 0.2[†]
Dextromethorphan	36.6 ± 2.3*	21.1 ± 3.8*,[†]

Abbreviations: fMLP, N-formyl-methionyl-leucyl-phenylalanine; PMA, phorbol-12-myristate-13-acetate; ROS, reactive oxygen species.
ROS were measured by lucigenin-amplified chemiluminescence, and values of the IC_{50} for dimemorfan, BD1047, dimemorfan + BD1047 (20 μM) and dextromethorphan were determined. Data are expressed as the mean ± s.e.mean ($n = 5$–8 for each group). *$P < 0.05$, compared with dimemorfan + BD1047 group and [†]$P < 0.05$, compared with PMA group by one-way ANOVA followed by the Student–Newman–Keuls t-test.
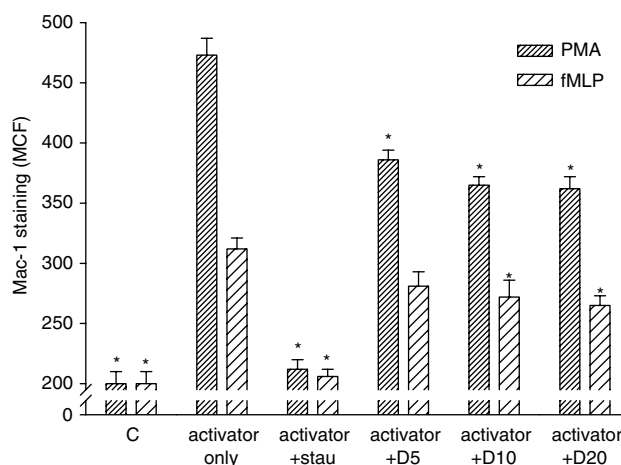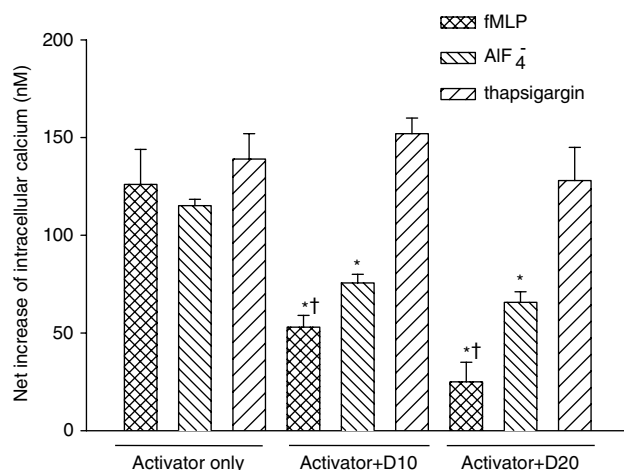
Figure 2 Effects of dimemorfan on increased intracellular calcium concentration, induced by different activators, in human neutrophils. Changes of intracellular calcium concentration in fura-2 AM preloaded human neutrophils (2×10^7 cells mL^{-1}) pre-treated with 10 or 20 μM dimemorfan ($+$D10 or $+$D20) were measured after stimulation with N-formyl-methionyl-leucyl-phenylalanine (fMLP, 1 μM), AlF$_4^-$ (10 mM NaF plus 30 μM AlCl$_3$), or thapsigargin (10 μM). Net increase of intracellular calcium concentration (nM) ($\Delta[Ca^{2+}]_i$) was calculated by subtraction of the value of $[Ca^{2+}]_i$ in resting cells (82 ± 3.0 nM) from each data point. Data are expressed as the mean $\pm$ s.e.m. ($n = 3$–5 for each group). *$P < 0.05$, compared with the corresponding activator only group, $^\dagger P < 0.05$, compared with AlF$_4^-$ $+$D10 or AlF$_4^-$ $+$D20, respectively, by one-way ANOVA followed by the Student-Newman-Keuls t-test.

(one-way ANOVA, $P < 0.05$). The positive controls including trolox (50 μM, an antioxidant) and N^G-nitro-L-arginine methyl ester (L-NAME, 20 μM, a NOS inhibitor) significantly reduced LPS-stimulated ROS and NO production, respectively. A NF-κB inhibitor, pyrrolidine dithiocarbamate (PDTC, 10 μM) also significantly reduced LPS-stimulated NO production (Figure 3). Dimemorfan (10–20 μM) alone had no effects on either ROS or NO production (data not shown).

Effects on iNOS expression and NOX activity

To examine whether the inhibitory effects of dimemorfan on NO and ROS production is due to inhibition of iNOS upregulation and NOX activity, respectively, iNOS expression in LPS-activated BV2 cells and NOX activity in cell free system were examined. LPS (0.5 μg mL^{-1}) dramatically increased iNOS protein expression at 24 h after LPS treatment (Figure 4), but non-activated cells (LPS free, Figure 4) or treatment of dimemorfan alone (data not shown) did not stimulate iNOS protein expression. Pre-treatment with dimemorfan (10–20 μM) significantly suppressed LPS-induced iNOS protein expression (Figure 4), possibly through inhibiting NF-κB phosphorylation (pp65)/activation (Figure 4). In addition, dimemorfan (10–50 μM) concentration-dependently inhibited NOX activity. The inhibition percentage ranged from 13 to 44% in BV2 cells and the IC$_{50}$ value was 47 μM in neutrophils (Table 2). Diphenylene iodonium, a potent NOX inhibitor used as a positive control, significantly blocked NOX activity with IC$_{50}$ values of 12 and 24 μM for BV2 and neutrophils, respectively (Table 2).
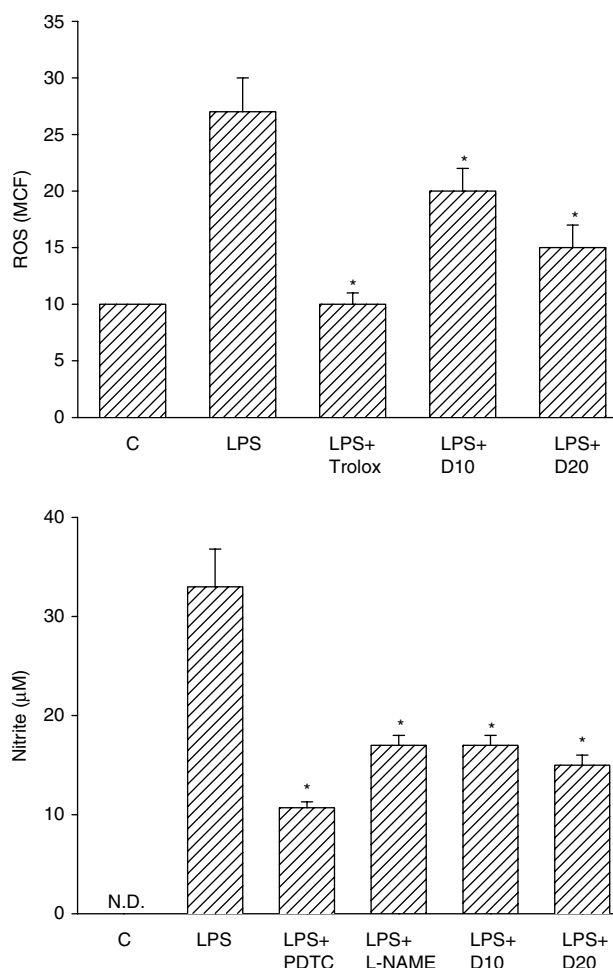

Figure 3 Effects of dimemorfan on lipopolysaccharide (LPS)-induced reactive oxygen species (ROS) (upper panel) and NO production (lower panel) in murine microglial cells. ROS (mean channel fluorescence, MCF) or NO (nitrite, μM) production in cells pre-treated with solvent (LPS) or 10–20 μM of dimemorfan (LPS $+$ D10 or LPS $+$ D20) was measured after stimulation with LPS (0.5 μg mL^{-1}) for 24 h. Cells in control group (C) received solvent only (drug free). Trolox (an antioxidant, 50 μM), pyrrolidinethiocarbamate (PDTC, a NF-κB inhibitor, 10 μM) and L-NAME (an NOS inhibitor, 20 μM) were used as positive controls. Data are expressed as the mean $\pm$ s.e.m. ($n = 6$–10 for each group). *$P < 0.05$, compared with the LPS only group by one-way ANOVA followed by the Student-Newman-Keuls t-test. N.D., not detectable.

Effects on MCP-1 and TNF-α production in BV2 cells

To examine whether dimemorfan could suppress the production of pro-inflammatory cytokines, LPS-stimulated production of MCP-1 and TNF-α were evaluated in BV2 cells. Using an intracellular cytokine staining method, we found that only a small population (2.5–3.6%) of BV2 cells revealed positive staining of MCP-1 or TNF-α in a resting condition. Stimulation of BV2 cells with LPS (0.5 μg mL^{-1}) dramatically increased the proportion of cells staining for MCP-1 or TNF-α to around 25.3 and 75.4%, respectively (Table 3). The relative content of MCP-1 and TNF-α in the positively stained BV2 cytosol, as estimated by the MCF intensity, also increased by 2.4- and 4.6-fold, respectively (Table 3). Pretreatment with dimemorfan (10–20 μM) significantly suppressed both the percentage of the positively

stained population and the MCF intensities of MCP-1 and TNF-α in BV2 cytosol (one-way ANOVA, $P < 0.05$). PDTC significantly blocked the increment in the percentage of the positively stained cell population and the MCF intensities of MCP-1 and TNF-α in BV2 cytosol (one-way ANOVA, $P < 0.05$).

Effect on NF-κB signalling and activity
To examine whether NF-κB signalling was modulated by dimemorfan, the effects of dimemorfan on LPS-induced nuclear translocation of NF-κB p65 and degradation of

cytosolic Iκ-Bα, an NF-κB inhibitor protein, as well as the transcriptional activity of NF-κB in BV2 cells were examined. LPS induced significant degradation of cytosolic Iκ-Bα (Figure 5) and nuclear translocation of NF-κB p65 (Figure 5), and dramatically enhanced the transcriptional activity of NF-κB in BV2 cells (Figure 6). Dimemorfan (20 μM) significantly blocked the degradation of cytosolic Iκ-Bα (Figure 5) and nuclear translocation of NF-κB p65, as well as the transcriptional activity of NF-κB (Figure 6). These results suggest that dimemorfan inhibits the NF-κB signalling pathway in LPS-stimulated BV2 cells.
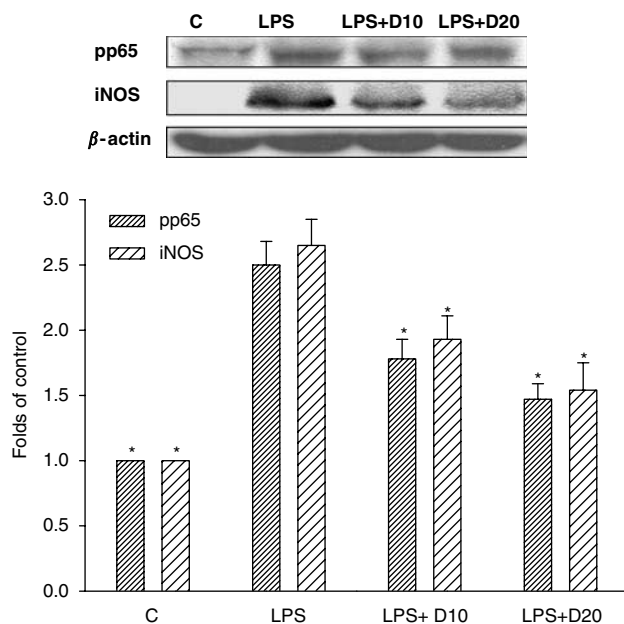

Figure 4 Effects of dimemorfan on lipopolysaccharide (LPS)-induced phospho-NF-κB p65 (pp65) and inducible nitric oxide synthase (iNOS) expression in murine microglial cells at 24 h. The upper panel shows representative immunoblots of pp65 and iNOS in microglial cells pre-treated with solvent only (LPS), 10 or 20 μM of dimemorfan (LPS + D10 or LPS + D20) followed by stimulation with LPS (0.5 μg mL^{-1}). Cells in control group (C) received solvent only (drug free). The β-actin signal was used as a reference for protein normalization. The lower panel shows the statistical results (mean ± s.e.m., $n = 3–5$) of the densitometric measurements after normalization to β-actin. *$P < 0.05$, compared with the corresponding LPS only group by one-way ANOVA followed by the Student-Newman-Keuls *t*-test.

Effect on LPS-induced endotoxin shock in mice
Dimemorfan given three times after LPS (at 30 min, 6 and 12 h), protected mice against signs of endotoxin shock. Thus, plasma levels of TNF-α were markedly increased at 6 or 12 h after LPS alone and this increase was clearly suppressed by dimemorfan (Figure 7, one-way ANOVA, $P < 0.05$). Similarly, the infiltration of neutrophils into lung and liver as well as the production of oxidative stress (EB staining) in these tissues induced by LPS was markedly inhibited by the treatment with dimemorfan (Figure 8, one-way ANOVA, $P < 0.05$). Survival of mice at 48 h after the LPS injection was also significantly increased by dimemorfan (data not shown).

Table 2 Effects of dimemorfan on NOX activity from BV2 cells and human neutrophils

Treatment	Maximum inhibition (%) in BV2 cells	IC$_{50}$ (μM) in neutrophils
Dimemorfan	44 ± 2*	47 ± 3*
Diphenylene iodonium	90 ± 5	24 ± 5

Abbreviation: NOX, NADPH oxidase.
Cell lysate from BV2 cells and human neutrophils was co-incubated with 10–50 μM of dimemorfan in the presence of lucigenin (50 μM) and NADPH (200 μM). NOX activity was determined from the chemiluminescence. Data are calculated as the IC$_{50}$ or the percent of maximum inhibition at 50 μM when IC$_{50}$ value is not obtainable, and expressed as the mean ± s.e.mean of five to six experiments performed on different days using cells from different passages (BV2) or healthy donors (neutrophils). *$P < 0.05$, compared with diphenylene iodonium group, by *t*-test.

Table 3 Effects of dimemorfan on LPS-induced production of MCP-1 and TNF-α in murine microglial cells

Treatment	MCP-1		TNF-α	
	%	MCF	%	MCF
Control (drug free)	2.5 ± 0.3*	14.5 ± 2.0*	3.6 ± 0.6*	43.5 ± 2.2*
LPS (0.5 μg mL^{-1})	25.3 ± 4.5	34.2 ± 2.9	75.4 ± 2.0	200.0 ± 11.8
+ dimemorfan (10 μM)	19.7 ± 3.0	29.4 ± 4.6	64.8 ± 2.3*	168.8 ± 9.0*
+ dimemorfan (20 μM)	11.8 ± 3.6*	22.2 ± 2.5*	63.0 ± 2.6*	161.5 ± 9.4*
+ pyrrolidine dithiocarbamate (20 μM)	10.5 ± 4.2*	20.7 ± 4.8*	45.2 ± 5.5*	119.6 ± 10.1*

Abbreviations: LPS, lipopolysaccharide; MCF, mean channel fluorescence; MCP-1; monocyte chemoattractant protein-1; PMA, phorbol-12-myristate-13-acetate; ROS, reactive oxygen species; TNF-α, tumour necrosis factor-α.
MCP-1 or TNF-α production induced by LPS (0.5 μg mL^{-1}) for 4 h was measured by an intracellular staining method and estimated by the percentage of positively stained cells (%) and MCF in positively stained cells of BV2 cells with or without pretreatment with dimemorfan (10 or 20 μM). Pyrrolidine dithiocarbamate (an NF-κB inhibitor) was used as a positive control. Data are expressed as the mean ± s.e.mean ($n = 6–10$ for each group). *$P < 0.05$, compared with LPS only group by one-way ANOVA followed by the Student–Newman–Keuls *t*-test.
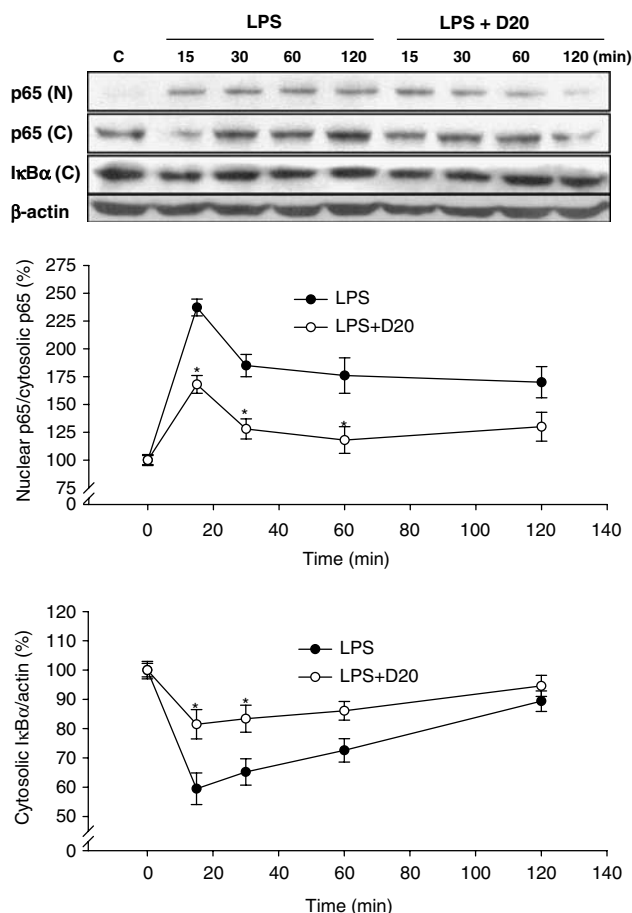
Figure 5 Effects of dimemorfan on the lipopolysaccharide (LPS)-induced nuclear translocation of NF-κB p65 and degradation of cytosolic IκBα in murine microglial cells. The upper panel shows representative immunoblots of time-dependent translocation of NF-κB p65 from the cytosol (p65 (C)) to the nucleus (p65 (N)) and degradation of cytosolic IκBα (IκBα (C)) in microglial cells pre-treated with solvent only (LPS) or 20 μM of dimemorfan (LPS + D20) followed by stimulation with LPS (0.5 μg mL^{-1}) for different times (from 15 to 120 min). Cells in control group (C) received solvent only (drug free). The β-actin signal was used as a reference for IκBα normalization. The lower panel shows the statistical results (mean ± s.e.m., $n = 3$) of the densitometric measurements after normalization of p65 (N) and IκBα (C) to p65 (C)) and β-actin, respectively. *$P < 0.05$, compared with LPS only group at the indicated time point by one-way ANOVA followed by the Student-Newman-Keuls *t*-test.

Discussion

The prompt and vigorous production of ROS, the so-called 'respiratory burst', and upregulated expression of firm adhesion molecules (e.g., β2 integrin Mac-1) are important inflammatory responses by human leukocytes (Shen *et al.*, 1999, 2002; Wang *et al.*, 2006). Besides, activation of microglial cells by bacterial endotoxins (e.g., LPS) and cytokines (e.g., interferon-γ) produces large amounts of NO and ROS that is accompanied by the induction of iNOS expression and activation of NOX, respectively, resulting in cell damage by NO or ROS and the toxic metabolite, peroxynitrite (ONOO$^-$) (Dringen, 2005; Li *et al.*, 2005; Wang *et al.*, 2006; Ko *et al.*, 2007). To elucidate whether the inhibitory effect on ROS and NO production by dimemorfan
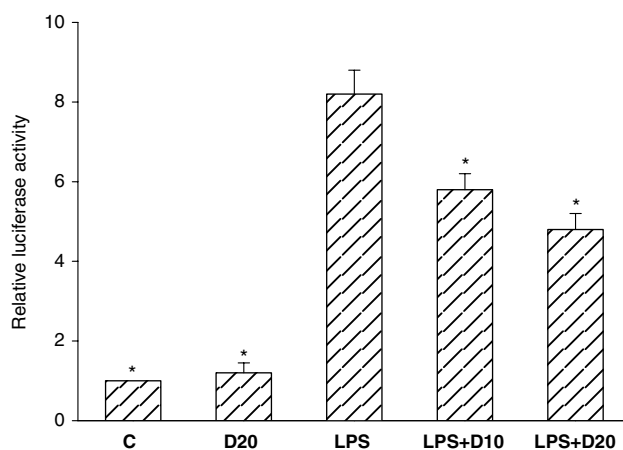

Figure 6 Effect of dimemorfan on lipopolysaccharide (LPS)-induced activation of the NF-κB-luciferase reporter in BV2 cells. Cells were co-transfected with the NF-κB-luciferase reporter gene and β-galactosidase vector and pre-treated with solvent (LPS) or 10 or 20 μM dimemorfan (LPS + D10 or LPS + D20) followed by stimulation with LPS (0.5 μg mL^{-1}) for 6 h. Cells in control groups received solvent only (C) or 20 μM dimemorfan only (D20). Luciferase activity was normalized to the transfection efficiency with the β-galactosidase expression vector. *$P < 0.05$, compared with LPS only group by one-way ANOVA followed by the Student-Newman-Keuls *t*-test.
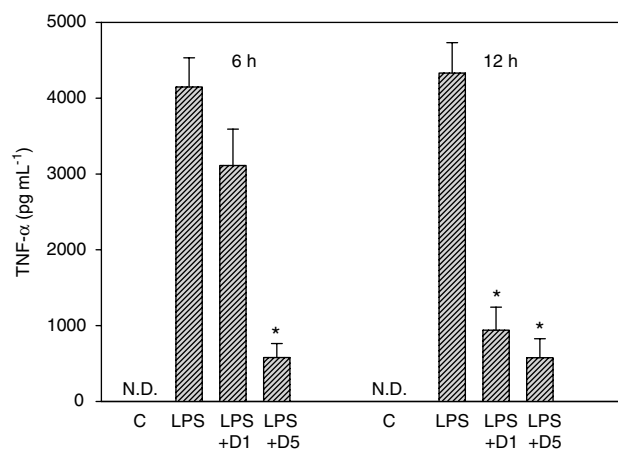

Figure 7 Effects of dimemorfan treatment on lipopolysaccharide (LPS)-induced increases in plasma TNF-α concentration in mice. After administration of LPS (70 mg kg^{-1}, i.p.), mice were injected with saline (shown as LPS), or dimemorfan (1 or 5 mg kg^{-1}, i.p.; LPS + D1 or LPS + D5) at 30 min, 6 and 12 h after the LPS. Mice in control group (C) received solvent only (drug free). The plasma TNF-α concentration (mean ± s.e.m., $n = 5$ for each group) was measured at 6 and 12 h after LPS administration. *$P < 0.05$, compared with LPS only group by one-way ANOVA followed by the Student-Newman-Keuls *t*-test. N.D., not detectable.

underlies its protective effect observed in animal models of inflammation-mediated disorders (Chou *et al.* 1999; Shin *et al.* 2005; Shen *et al.*, 2008), the effects of dimemorfan on PMA- and fMLP-induced ROS production and Mac-1 expression in peripheral human neutrophils, as well as ROS and NO production, iNOS expression, and NOX activity in microglial cells were examined. The results indicated that dimemorfan exerts an anti-inflammatory action through mechanisms independent of σ$_1$ receptors but involving an inhibition of
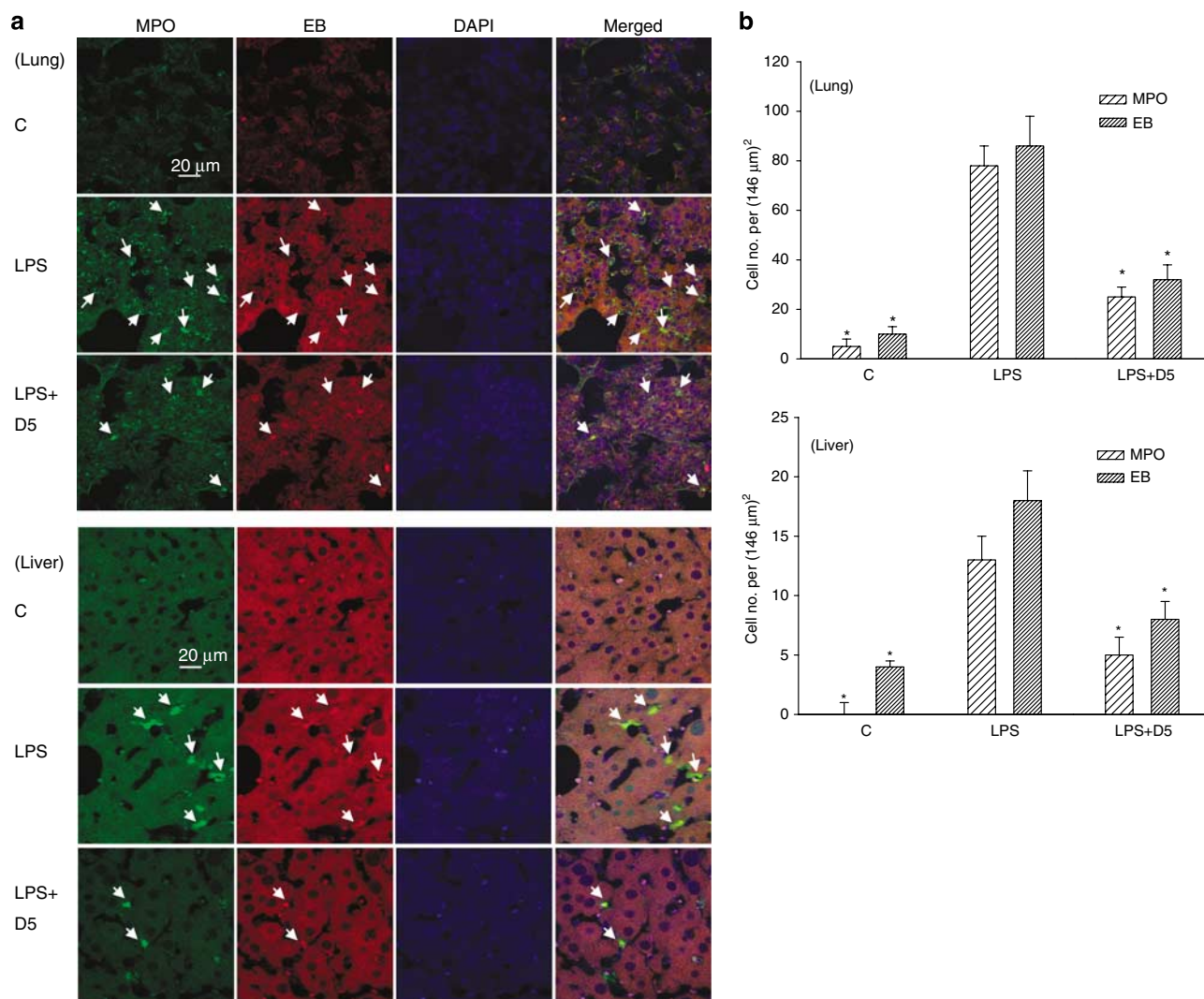
Figure 8 Effects of dimemorfan treatment on lipopolysaccharide (LPS)-induced increment in the neutrophil infiltration and production of oxidative stress in lung and liver at 48 h. (**a**) After administration of LPS (70 mg kg^{-1}, i.p.), mice were injected with saline (LPS) or 5 mg kg^{-1} (i.p.) of dimemorfan (LPS + D5) at 30 min, 6 and 12 h. Mice in control group (C) received solvent only (drug free). Neutrophil infiltration was revealed by positive staining for myeloperoxidase (MPO, green fluorescence) and oxidative stress was revealed by positive staining with ethidium (EB, red fluorescence). Arrows indicate the colocalization (yellow) of MPO staining and EB in the merged column. An appropriate dilution of 4′,6-diamidino-2-phenylindole (DAPI, blue) was used to counterstain DNA in the nuclei. (**b**) Statistical results from three to five independent experiments were calculated as the mean ± s.e.m. *$P < 0.05$, compared with the corresponding LPS only group by one-way ANOVA followed by the Student-Newman-Keuls *t*-test.

the increase in intracellular calcium concentration and a partial inhibition of NOX dependent ROS production, which in turn modulate the NF-κB-dependent upregulation of iNOS and NO production, as well as that of pro-inflammatory cytokine (TNF-α), to protect against inflammation-mediated disorders.

In this study, we used PMA, a protein kinase C activator, and fMLP, a synthetic bacterial peptide that activates leukocytes through a receptor-mediated pathway, to elucidate the mechanisms of action of dimemorfan on neutrophils. Production of ROS induced by PMA or fMLP were both significantly inhibited by dimemorfan with the greater potency against fMLP. In addition, dimemorfan was more potent in the inhibition of fMLP- than of G-protein (AlF$_4^-$)-induced increase in intracellular calcium concentration,

indicating that dimemorfan could interfere with the receptor-mediated G-protein signalling, other than signalling down stream of G-protein activation (protein kinase C activation). Protein kinase C plays a major role in mediating ROS production in neutrophils through phosphorylation and activation of p47^{phox}, an important cytosolic component of NOX (Casimir and Teahan, 1994; Selvatici *et al.*, 2006). Our previous report showed that the general protein kinase C inhibitors, GF109203x and staurosporine, both exhibited potent activity in inhibiting PMA- and fMLP-induced ROS production, indicating that protein kinase C is central to NOX activation (Wang *et al.*, 2004b). To further understand whether protein kinase C can be modulated by dimemorfan, pan-protein kinase C activity from the total cell lysate of human neutrophils was examined. We did not

observe significant inhibition of pan-protein kinase C activity by dimemorfan (data not shown), indicating that dimemorfan does not directly interfere with protein kinase C activity.

NOX is the major ROS-producing enzyme in activated leukocytes (Van den Worm et al., 2001). Drugs with anti-inflammatory activity have been reported to display potent NOX-inhibitory action (Liou et al., 2003; Lin et al., 2006). To further understand whether the inhibitory action on ROS production by dimemorfan is due to direct inhibition of NOX, the effects of dimemorfan on NOX activities in lysates of BV2 cells and human neutrophils were examined. Our data showed that dimemorfan is an inhibitor of NOX, with maximum (44%) inhibition of NOX activity at $50 \mu M$ in BV2 cells and an IC_{50} value of around $47 \mu M$ in neutrophils, although it is less potent than the well-known NOX inhibitor, diphenylene iodonium, with IC_{50} values around $12–24 \mu M$. Additionally, the inhibitory action of dimemorfan on ROS production was not due to direct free radical-scavenging capacity, because dimemorfan ($10–50 \mu M$) showed no significant free radical-scavenging activity in a DPPH free radicals system and in a cell-free xanthine/ xanthine oxidase system in which xanthine oxidase catalyses the oxidation of xanthine to produce uric acid as the final product, accompanied with the production of both superoxide anion and hydrogen peroxide (Wang et al., 2004b).

Activated leukocytes preferentially infiltrate and accumulate at sites of inflammation through upregulated expression of β2 integrins, especially Mac-1 (CD11b/CD18) to counteract its counter receptor, e.g., intercellular adhesion molecule-1 (ICAM-1), for firm adherence to vascular endothelium cells (Wang and Doerschuk, 2000; Wang et al., 2004b, 2006). They then transmigrate and infiltrate into injured tissue where they release hydrolytic enzymes and large amounts of ROS leading to overt tissue damage (Wardlaw and Walsh, 1994; Wang and Doerschuk, 2000). We have reported that intracellular ROS production and increase of intracellular calcium concentration are two important signals mediating leukocyte activation and upregulated expression of integrins (Shen et al., 1999). Dimemorfan significantly inhibited PMA- or fMLP-induced Mac-1 upregulated expression possibly by inhibiting ROS production and impeding intracellular calcium increase in neutrophils, suggesting that dimemorfan exhibits the ability to limit the infiltration of leukocytes into inflammatory tissue. This effect has been further confirmed in vivo by showing that dimemorfan treatment decreased neutrophil infiltration and oxidative stress production induced by LPS, in the lung and liver of mice.

Microglial cells are one of the most important immuno-effector cells in brain inflammatory responses which mediate neurodegeneration (Rong and Baudry, 1996; Van Eldik et al., 2007), while NO and ROS are also two important inflammatory mediators produced by activated microglial cells during inflammation (Shen et al., 2005; Kim et al., 2006; Shen et al., 2008). After stimulation of microglial cells with bacterial endotoxins (LPS) or cytokines (IFN-γ), production of NO and ROS is accompanied by the induction of iNOS and activation of NOX, respectively. These effects result in tissue damage by NO itself and its more toxic metabolite, $ONOO^-$ (Dringen,

2005; Li et al., 2005). We previously reported that antioxidant and anti-inflammatory drugs with inhibitory action on iNOS expression can prevent stroke-induced brain injury by limiting formation of $ONOO^-$ (Wang et al., 2006; Shen et al., 2008). It is now well-accepted that inhibiting NO production by interfering with iNOS expression, as well as inhibiting ROS production by impeding NOX activity is beneficial for treating inflammation-mediated disorders and neurodegenerative diseases (Di Rosa et al., 1990; Klegeris et al., 2007; Lau et al., 2007). As dimemorfan significantly reduced the production of both ROS and NO at 24 h after LPS induction in microglial cells, the formation of $ONOO^-$ could also be effectively prevented by dimemorfan. Furthermore, diminishing NO production by decreasing iNOS expression through inhibiting the activation of the NF-κB signalling pathway is an essential mechanism responsible for the effects of several anti-inflammatory drugs (Xie et al., 1994; Chen et al., 2000; Li et al., 2000; Takada et al., 2005; Lu et al., 2007). Dimemorfan significantly reduced NF-κB activation by suppressing p65 (RelA) phosphorylation and/or degradation of IκBα, and subsequently the nuclear translocation of p65, as well as the transcriptional activity of NF-κB. These effects could account for the inhibition of LPS-induced iNOS expression and NO production by dimemorfan.

Activated microglial cells release significant amounts of proinflammatory cytokines to further recruit and activate other immune cells. Pro-inflammatory cytokines (interleukin-1 and TNF-α) are downstream gene products of NF-κB signalling produced by microglia that exert synergistic effects in N-methyl-D-aspartate (NMDA)-mediated neurotoxicity (Chao et al., 1995). We found that LPS induced dramatic amounts of MCP-1 and TNF-α production in BV2 cells which were significantly reduced by dimemorfan. Because PDTC (a NF-κB inhibitor) significantly reduced cytokine release, the inhibitory effect of dimemorfan on pro-inflammatory cytokine production by microglial cells may be mediated through modulation of the IκB/NF-κB signalling pathway. The above mentioned effects of dimemorfan on inflammatory cells were not due to cytotoxicity, because no significant cell death was observed in the concentration ranges examined (data not shown).

In this study, the concentrations of dimemorfan ($10–20 \mu M$) having an inhibitory action on ROS production are much higher than the levels shown to inhibit the cough reflex through σ_1 receptors in human plasma ($0.007–0.008 \mu g \, mL^{-1}$) (Seki, 1972). However, this in vitro concentration appears to be comparable to the blood concentration of dimemorfan after the treatment used in the endotoxin shock model in mice ($1–5 \, mg \, kg^{-1}$, i.p., at three successive times). Although this in vivo dose is higher than those used in the antitussive activity of σ_1 receptor agonists in animals (Brown et al., 2004), but it was still within the safe and pharmacologically applicable dosage range. The maximum non-toxic dose in rats was $25 \, mg \, kg^{-1}$ per day in males and $50 \, mg \, kg^{-1}$ per day in females after 5 weeks oral administration, and $25 \, mg \, kg^{-1}$ per day in both sexes after 26 weeks oral administration. In other species, the maximum non-toxic dose was $50 \, mg \, kg^{-1}$ per day in male mice, $25 \, mg \, kg^{-1}$ per day in male guinea pigs, and $10 \, mg \, kg^{-1}$ per day in male dogs (Miki et al., 1972; Yoshida et al., 1972). Because σ_1 receptor

agonists have been reported to have anti-inflammatory effect (Bourrié et al., 2002, 2004), it is reasonable to speculate that dimemorfan should activate the σ_1 receptors to exhibit its anti-inflammatory effect. However, the present study demonstrated that the σ_1 receptor antagonist BD1047 itself had some inhibitory effect and potentiated dimemorfan's inhibition of ROS production in neutrophils, indicating that the σ_1 receptors were not involved in dimemorfan's effects. In addition, dextromethorphan, an analogueue of dimemorfan, has been reported to be beneficial in inflammation-mediated neurodegeneration through inhibition of microglial activation (Liu et al., 2003) and to prevent LPS-induced sepsis in rats by reduction in pro-inflammatory cytokine release (TNF-α) and suppression of NO production, and by its antioxidant properties (Wang et al., 2004a). Although dextromethorphan is effective in the inhibition of ROS production in neutrophils, it was less potent than dimemorfan in this study. Unlike dimemorfan, dextromethorphan is metabolized to dextrophan to cause phencyclidine-like behavioural side effects (Kase et al., 1976).

In conclusion, our results demonstrated that dimemorfan displays inhibitory activities on both ROS and NO production in inflammatory cells that allow it to be an effective anti-inflammatory drug in vivo. The anti-inflammatory properties of dimemorfan could be due, at least in part, to limiting NOX-dependent ROS and iNOS-dependent NO production, as well as pro-inflammatory cytokine release through modulation of intracellular calcium concentration and NF-κB signalling pathway in inflammatory cells. As a highly effective and widely used antitussive for more than 30 years, dimemorfan has an established safety record in humans, making it an attractive agent for further development in the treatment of inflammation-related disorders.

Acknowledgements

Conflict of interest

The authors state no conflict of interest.

References

Ajmo Jr CT, Vernon DO, Collier L, Pennypacker KR, Cuevas J (2006). Sigma receptor activation reduces infarct size at 24 h after permanent middle cerebral artery occlusion in rats. Curr Neurovasc Res 3: 89–98.

Bourrié B, Bribes E, De Nys N, Esclangon M, Garcia L, Galiègue S et al. (2002). SSR125329A, a high affinity sigma receptor ligand with potent anti-inflammatory properties. Eur J Pharmacol 456: 123–131.

Bourrié B, Bribes E, Derocq JM, Vidal H, Casellas P (2004). Sigma receptor ligands: applications in inflammation and oncology. Curr Opin Investig Drugs 5: 1158–1163.

Brown C, Fezoui M, Selig WM, Schwartz CE, Ellis JL (2004). Antitussive activity of sigma-1 receptor agonists in the guinea-pig. Br J Pharmacol 141: 233–240.

Casimir CM, Teahan CG (1994). The respiratory burst of neutrophils and its deficiency. In: Hellewell PG, Williams TJ (eds). Immunopharmacology of Neutrophils. Academic Press: San Diego, pp 27–54.

Chao CC, Hu S, Ehrlich L, Peterson PK (1995). Interleukin-1 and tumor necrosis factor-alpha synergistically mediate neurotoxicity: involvement of nitric oxide and of N-methyl-D-aspartate receptors. Brain Behav Immun 9: 355–365.

Chen Y, Yang L, Lee TJ (2000). Oroxylin A inhibition of lipopolysaccharide-induced iNOS and COX-2 gene expression via suppression of nuclear factor-kappaB activation. Biochem Pharmacol 59: 1445–1457.

Chou YC, Liao JF, Chang WY, Lin MF, Chen CF (1999). Binding of dimemorfan to sigma-1 receptor and its anticonvulsant and locomotor effects in mice, compared with dextromethorphan and dextrorphan. Brain Res 821: 516–519.

Di Francesco P, Falchetti R, Gaziano R, Lanzilli G, Casalinuovo IA, Ravagnan G et al. (1999). Effects of cocaine administration to influenza virus-immunized mice on cytokine profiles of individual splenic CD4$^+$ and CD8$^+$ T cells. Clin Exp Immunol 118: 428–434.

Di Rosa M, Radomski M, Carnuccio R, Moncada S (1990). Glucocorticoids inhibit the induction of nitric oxide synthase in macrophages. Biochem Biophys Res Commun 172: 1246–1252.

Dringen R (2005). Oxidative and antioxidative potential of brain microglial cells. Antioxid Redox Signal 7: 1223–1233.

Falchetti R, Fuggetta MP, Lanzilli G, Tricarico M, Ravagnan G (2001). Effects of resveratrol on human immune cell function. Life Sci 70: 81–96.

Gannon CJ, Malone DL, Napolitano LM (2001). Reduction of IL-10 and nitric oxide synthesis by SR31747A (sigma ligand) in RAW murine macrophages. Surg Infect 2: 267–272.

Ghoshal A, Das S, Ghosh S, Mishra MK, Sharma V, Koli P et al. (2007). Proinflammatory mediators released by activated microglia induces neuronal death in Japanese encephalitis. Glia 55: 483–496.

Jiau SS, Cheng PY, Lee YM, Huang WH, Ko YF, Yen MH (2006). Beneficial effects of LK-4, an analog of dextromethorphan on lipopolysaccharide-induced sepsis in rats. J Biomed Sci 13: 833–843.

Kase Y, Kito G, Miyata T, Uno T, Takahama K, Ida H (1976). Antitussive activity and other related pharmacological properties of d-3-methyl-N-methylmorphinan (AT-17). Arzneim-Forsch (Drug Res) 26: 353–360.

Kim JS, Lee HJ, Lee MH, Kim J, Jin C, Ryu JH (2006). Luteolin inhibits LPS-stimulated inducible nitric oxide synthase expression in BV-2 microglial cells. Planta Med 72: 65–68.

Klegeris A, McGeer EG, McGeer PL (2007). Therapeutic approaches to inflammation in neurodegenerative disease. Curr Opin Neurol 20: 351–357.

Ko HC, Wang YH, Liou KT, Chen CM, Chen CH, Wang WY et al. (2007). Anti-inflammatory effects and mechanisms of the ethanol extract of Evodia rutaecarpa and its bioactive components on neutrophils and microglial cells. Eur J Pharmacol 555: 211–217.

Kodama T, Yukioka H, Kato T, Kato N, Hato F, Kitagawa S (2007). Neutrophil elastase as a predicting factor for development of acute lung injury. Intern Med 46: 699–704.

Lau FC, Bielinski DF, Joseph JA (2007). Inhibitory effects of blueberry extract on the production of inflammatory mediators in lipopolysaccharide-activated BV2 microglia. J Neurosci Res 85: 1010–1017.

Li J, Baud O, Vartanian T, Volpe JJ, Rosenberg PA (2005). Peroxynitrite generated by inducible nitric oxide synthase and NADPH oxidase mediates microglial toxicity to oligodendrocytes. Proc Natl Acad Sci USA 102: 9936–9941.

Li YH, Yan ZQ, Jensen JS, Tullus K, Branner A (2000). Activation of nuclear factor-κB and induction of inducible nitric oxide synthase by Ureaplasma urealyticum in macrophages. Infect Immun 68: 7087–7093.

Lin LC, Wang YH, Hou YC, Chang S, Liou KT, Chou YC et al. (2006). The inhibitory effect of phenylpropanoid glycosides and iridoid glucosides on free radical production and beta2 integrin expression in human leukocytes. J Pharm Pharmacol 58: 129–135.

Liou KT, Shen YC, Chen CF, Tsao CM, Tsai SK (2003). The anti-inflammatory effect of honokiol on neutrophils: mechanisms in

the inhibition of reactive oxygen species production. *Eur J Pharmacol* **475**: 19–27.

Liu Y, Qin L, Li G, Zhang W, An L, Liu B et al. (2003). Dextromethorphan protects dopaminergic neurons against inflammation-mediated degeneration through inhibition of microglial activation. *J Pharmacol Exp Ther* **305**: 212–218.

Lu DY, Tang CH, Liou HC, Teng CM, Jeng KC, Kuo SC et al. (2007). YC-1 attenuates LPS-induced proinflammatory responses and activation of nuclear factor-kappaB in microglia. *Br J Pharmacol* **151**: 396–405.

Mattson MP, Camandola S (2001). NF-kappa B in neuronal plasticity and neurodegenerative disorders. *J Clin Invest* **107**: 247–254.

Miki N, Yoshida T, Kotani Y, Sado T (1972). Effects of a new antitussive agent, d-3-methyl-N-methylmorphinan phosphate (AT-17), on the liver and pancreas of several species of experimental animals. *Clin Rep* **6**: 2104–2109.

Muir KW, Tyrrell P, Sattar N, Warburton E (2007). Inflammation and ischaemic stroke. *Curr Opin Neurol* **20**: 334–342.

Nathan C (2002). Points of control in inflammation. *Nature* **420**: 846–852.

Rogers J, Mastroeni D, Leonard B, Joyce J, Grover A (2007). Neuroinflammation in Alzheimer's disease and Parkinson's disease: Are microglia pathogenic in either disorder? *Int Rev Neurobiol* **82**: 235–246.

Rong Y, Baudry M (1996). Seizure activity results in a rapid induction of nuclear factor-kappa B in adult but not juvenile rat limbic structures. *J Neurochem* **67**: 662–668.

Seki T (1972). Measurement of plasma level of AT-17, a new antitussive agent, in human subjects. *Rinsho Yakuri* **3**: 302–304.

Selvatici R, Falzarano S, Mollica A, Spisani S (2006). Signal transduction pathways triggered by selective formylpeptide analogues in human neutrophils. *Eur J Pharmacol* **534**: 1–11.

Shen S, Yu S, Binek J, Chalimoniuk M, Zhang X, Lo SC et al. (2005). Distinct signaling pathways for induction of type II NOS by IFNgamma and LPS in BV-2 microglial cells. *Neurochem Int* **47**: 298–307.

Shen YC, Chen CF, Chiou WF (2002). Andrographolide prevents oxygen radical production by human neutrophils: possible mechanism(s) involved in its anti-inflammatory effect. *Br J Pharmacol* **135**: 399–406.

Shen YC, Chen CF, Wang SY, Sung YJ (1999). Impediment to calcium influx and reactive oxygen production accounts for the inhibition of neutrophil Mac-1 up-regulation and adhesion by tetrandrine. *Mol Pharmacol* **55**: 186–193.

Shen YC, Chiou WF, Chou YC, Chen CF (2003). Mechanisms in mediating the anti-inflammatory effects of baicalin and baicalein in human leukocytes. *Eur J Pharmacol* **465**: 171–181.

Shen YC, Sung YJ, Chen CF (1998). Magnolol inhibits Mac-1 (CD11b/CD18)-dependent neutrophil adhesion: relationship with its antioxidant effect. *Eur J Pharmacol* **343**: 79–86.

Shen YC, Wang YH, Chou YC, Liou KT, Yen JC, Wang WY et al. (2008). Dimemorfan protects rats against ischemic stroke through activation of sigma-1 receptor-mediated mechanisms by decreasing glutamate accumulation. *J Neurochem* **104**: 558–572.

Shin EJ, Nah SY, Kim WK, Ko KH, Jhoo WK, Lim YK et al. (2005). The dextromethorphan analog dimemorfan attenuates kainate-induced seizures via σ_1 receptor activation: comparison with the effects of dextromethorphan. *Br J Pharmacol* **144**: 908–918.

Takada Y, Kobayashi Y, Aggarwal BB (2005). Evodiamine abolishes constitutive and inducible NF-kappaB activation by inhibiting IkappaBalpha kinase activation, thereby suppressing NF-kappaB-regulated antiapoptotic and metastatic gene expression, up-regulating apoptosis, and inhibiting invasion. *J Biol Chem* **280**: 17203–17212.

Van den Worm E, Beukelman CJ, Van den Berg AJ, Kroes BH, Labadie RP, Van Dijk H (2001). Effects of methoxylation of apocynin and analogs on the inhibition of reactive oxygen species production by stimulated human neutrophils. *Eur J Pharmacol* **433**: 225–230.

Van Eldik LJ, Thompson WL, Ralay Ranaivo H, Behanna HA, Martin Watterson D (2007). Glia proinflammatory cytokine upregulation as a therapeutic target for neurodegenerative diseases: function-based and target-based discovery approaches. *Int Rev Neurobiol* **82**: 277–296.

Wang CC, Lee YM, Wei HP, Chu CC, Yen MH (2004a). Dextromethorphan prevents circulatory failure in rats with endotoxemia. *J Biomed Sci* **11**: 739–747.

Wang HH, Chien JW, Chou YC, Liao JF, Chen CF (2003). Anti-amnesic effect of dimemorfan in mice. *Br J Pharmacol* **138**: 941–949.

Wang Q, Doerschuk CM (2000). Neutrophil-induced changes in the biomechanical properties of endothelial cells: roles of ICAM-1 and reactive oxygen species. *J Immunol* **164**: 6487–6494.

Wang YH, Wang WY, Chang CC, Liou KT, Sung YJ, Liao JF et al. (2006). Taxifolin ameliorates cerebral ischemia-reperfusion injury in rats through its anti-oxidative effect and modulation of NF-kappa B activation. *J Biomed Sci* **13**: 127–141.

Wang YH, Wang WY, Liao JF, Chen CF, Hou YC, Liou KT et al. (2004b). Prevention of macrophage adhesion molecule-1 (Mac-1)-dependent neutrophil firm adhesion by taxifolin through impairment of protein kinase-dependent NADPH oxidase activation and antagonism of G protein-mediated calcium influx. *Biochem Pharmacol* **67**: 2251–2262.

Wardlaw AJ, Walsh GM (1994). Neutrophil adhesion receptor. In: Hellewell, PG, Williams TJ (eds). *Immunopharmacology of Neutrophils*. Academic Press: San Diego, pp 134–137.

Williams AJ, Dave JR, Tortella FC (2006). Neuroprotection with the proteasome inhibitor MLN519 in focal ischemic brain injury: relation to nuclear factor kappa B (NF-κB), inflammatory gene expression, and leukocyte infiltration. *Neurochem Int* **49**: 106–112.

Williams FM (1994). Role of neutrophils in reperfusion injury. In: Hellewell, PG, Williams TJ (eds). *Immunopharmacology of Neutrophils*. Academic Press: San Diego, pp 245–257.

Xie QW, Kashiwabara Y, Nathan C (1994). Role of transcription factor NF-κB/Rel in induction of nitric oxide synthase. *J Biol Chem* **269**: 4705–4708.

Yoshida T, Miki N, Sado T (1972). Toxicological studies of a new antitussive agent, d-3-methyl-N-methylmorphinan phosphate (AT-17). Part 1: Subacute and chronic toxicity tests on rats following oral drug administration. *Clin Rep* **6**: 2071–2090.